Modulation Analysis in Macro-Molecular Communications

DANIEL TUNÇ MCGUINESS[1], STAMATIOS GIANNOUKOS [1,2], ALAN MARSHALL[1] (Senior Member, IEEE), and STEPHEN TAYLOR[1]
[1]Department of Electrical Engineering and Electronics University of Liverpool Liverpool UK
[2]Laboratory of Atmospheric Chemistry, Paul Scherrer Institute, 5232 Villigen, Switzerland

Corresponding author: Daniel Tunç McGuiness (e-mail: danielmc@liverpool.ac.uk).

The research was funded from the Engineering and Physical Sciences Research Council (EPSRC) under the grant agreement: EP/M029425/1 'Creating a Stink - Investigating Olfactory Transport Streams'

ABSTRACT Molecular communication (MC) involves the transmission of information using particles (i.e., molecules). Research into the field have been dominated by micro-scale and most of the effects of macro-scale communication have yet to be studied. In this paper the modulation and transmission of molecular communication at macro-scale is investigated. As the transmitter, an in-house-built odor generator was used, and as the detector a mass spectrometer (MS) with a quadrupole mass analyzer (QMA) was employed. Various 2-level, 4-level and 8- level modulation schemes were tested experimentally. A simulation framework, developed for the first time, was used for a comparison with the experimental results. It was shown that the communication can be modeled using a variant of the advection-diffusion equation and that it gives good agreement with the experimental results. A symbol-error-rate (SER) analysis of both the experimental and simulation results was analyzed. It was found that increasing the distance has a detrimental effect on both the channel capacity and the SER, whereas velocity and diffusivity have a decreasing effect on the SER and an increasing effect on the channel capacity. A channel model was developed based on the asymmetric behavior of the communications and the optimal sampling period was developed that subsequently permitted analysis of the ISI of the communications scheme.

INDEX TERMS Macro-scale, mass spectrometer, asymmetric channel, bit-error rate, molecular inter-symbol interference

I. INTRODUCTION

MOLECULAR communications is an emerging field where information is conveyed using particles instead of electromagnetic (EM) waves. The information is encoded in the properties of the particles (type, quantity, release time) instead of a wave (amplitude, frequency). This change in the way information is transmitted is influenced by the communication methods already present in nature, which can be seen on both the macro-scale (i.e., the social interactions of insects using pheromones [1]–[3]) and the nano-scale (i.e., chemical signalling in intra-cellular communications [4]–[6]) environments.

Most studies of molecular communications have been made on the micro-scale, in the range of nm to μm [7]. These include modelling of the communication channel [8]–[10], error correction [11]–[13] and modulation [14]–[18]. There are applications of this range; such as its utilization of drug delivery systems/medicine [19]–[24] and nano scale robots [25]–[27].

At the macro-scale (cm - m), the range of the length opens up new possibilities. One notable area is to imitate and to study the behaviour of communications in nature using pheromones [28]–[32]. Experimentally, the idea of using chemicals as a means of communication has been shown as a proof of concept in [33], and in [34] it was shown that the transmission of information can be conducted over distances of up 3 m, and by utilizing a mass spectrometer, multiple chemicals can be sent and retrieved simultaneously. A recent experimental study was conducted in [35] where the possibility of macro-scale molecular communication was demonstrated using two types of modulation: On-off keying (OOK) and Concentration Shift Keying (CSK). Other experimental setups designed to analyze molecular communications on the macro-scale have also been reported [36]–[39].

There are various challenges associated with macro-scale communications compared to micro-scale, the main one being propagation. In the μm scale, the transmission can rely solely on the random motion of particles (diffusion), and the effect can be explained using Fick's 2nd Law of diffusion [40]. However, when communications are scaled up from

the μm range to metres, diffusion alone is not enough to propagate the particles. In order to increase the throughput of the communication, an additional flow is required to aid the transmission. However, most of literature regarding molecular communications is based on using diffusion as the means of propagation [41]–[52]. The study of advection with the addition of diffusion is seldom studied. In this paper it is used as the propagation method.

Another aspect of molecular communications is the left-over chemicals from previous transmissions. These can influence the next symbol and can cause incorrect decoding of the received bits and decrease the channel capacity. There have been studies on the micro-scale where modulation techniques were developed to reduce the effects on the communication [17], [18], [53]–[56] and the effects of ISI on other properties of molecular communications [57], [58]. A statistical study was also undertaken [59] .

In this paper both experimental and theoretical modulation analyses of macro-scale molecular communications are conducted. The experimental studies were made on the M-ary M = 2 (i.e., 0, 1), M = 4 (i.e., 00, 01, 10, 11) and M = 8 level transmission. A simulation model is developed based on the advection-diffusion equation to explain the behaviour of particle propagation in a medium and shows agreement with the experimental results. A SER study of molecular communications of 2-ary modulation is also tested. In addition, a theoretical analysis of an SER study was also conducted based on the simulation model, which also shows the consistency with the experimental results. Molecular inter-symbol interference (Mo-ISI) is discussed and an optimal transmission duration is calculated. Finally, a channel model is developed to explain the asymmetrical nature of the communications.

The major contributions of the paper are as follows;

1) **A simulation framework:** A model was developed to simulate an entire macro-scale communication, based on a variation of the mass transport equation called the advection-diffusion equation.
2) **M-ary Transmission study:** A comparison was made with experimental data of M-ary transmission of three levels (M = 2, M = 4 and M = 8) and for three different symbol periods (T_s = 30 s , T_s = 60 s and T_s = 90 s) which shows that the simulation framework can be used to model molecular communications at the macro-scale.
3) **Molecular ISI (Mo-ISI):** A study was made to analyze the effects of molecular ISI (Mo-ISI) in macro-scale molecular communications. The model developed is shown to have strong agreement with the experimental results. Mathematical equations were derived from the model to analytically calculate the residual chemicals from different types of transmissions.
4) **Optimal Symbol Duration:** An optimal symbol duration time is calculated by maximizing the error function used in the solution for the advection-diffusion equation.
5) **M-ary SER Analysis:** An SER analysis was conducted both experimentally (M = 2) and theoretically (M = 2, 4, 8, 16 and 32).
6) **Molecular Channel:** The type of the channel is defined as asymmetric and the capacity of the communication is described based on the asymmetric nature of the communication.
7) **Parameter effect on SER, MI and Distribution of Received Symbol Values:** A theoretical study of the mutual information (MI), SER and distribution of received symbol values was made on the three parameters: transmission distance (x), diffusivity (D) and advective flow (u_x)

The structure of the paper is as follows: In Section I an introduction to the subject and the study is presented. In Section II the experimental setup used in the M-ary transmission, SER study and molecular ISI is discussed in detail. Then in Section III, the mathematical model of the propagation and the simulation framework for molecular signal modulation is described based on the advection-diffusion. In Section IV the experimental results along with theoretical comparisons are described for the M-ary transmission. In Section V, molecular ISI is studied. Two types of experiments were conducted (k and o/z) and analyzed with the theoretical model developed in Section III. Section VI discusses the experimental analysis of M = 2 modulation along with theoretical comparisons to M = 2, M = 4 and M = 8. In Section VII the channel capacity is described and mutual information is calculated. In Section VIII the effects of various parameters on the achievable mutual information and SER are simulated based on the framework mentioned in Section III. In Section IX an analysis was made on the symbol distribution of a 4-ary transmission and the variance (σ^2) of the symbols is discussed. The paper ends with conclusions and future work in Section X.

II. EXPERIMENTAL SETUP

In this study, the modulation properties of M-ary transmission were investigated both experimentally and theoretically. The transmission of the 2-ary, 4-ary and 8-ary transmissions with symbol periods of T = 90 s, T = 60 s and T = 30 s were made experimentally along with the theoretical comparisons. All the experiments were made in the open air, where there is no closed boundary between the transmitter and the receiver, and the distance is x = 2.5 cm.

To test the modulation properties of the communication method in a macro-scale environment, a transmitter and a receiver are employed. The signal is generated by using an in-house-built odor generator. The detection was made with a mass spectrometer that uses a quadrupole mass analyzer (QMA). The mass spectrometer is an analytical device that can differentiate a given chemical by means of its mass-to-charge (m/z) ratio. The ability to separate and analyze chemicals in a given sample makes the MS a useful detector for MC. The experimental setup for both M-ary experiments and the symbol error rate (SER) is shown in Figure 1.

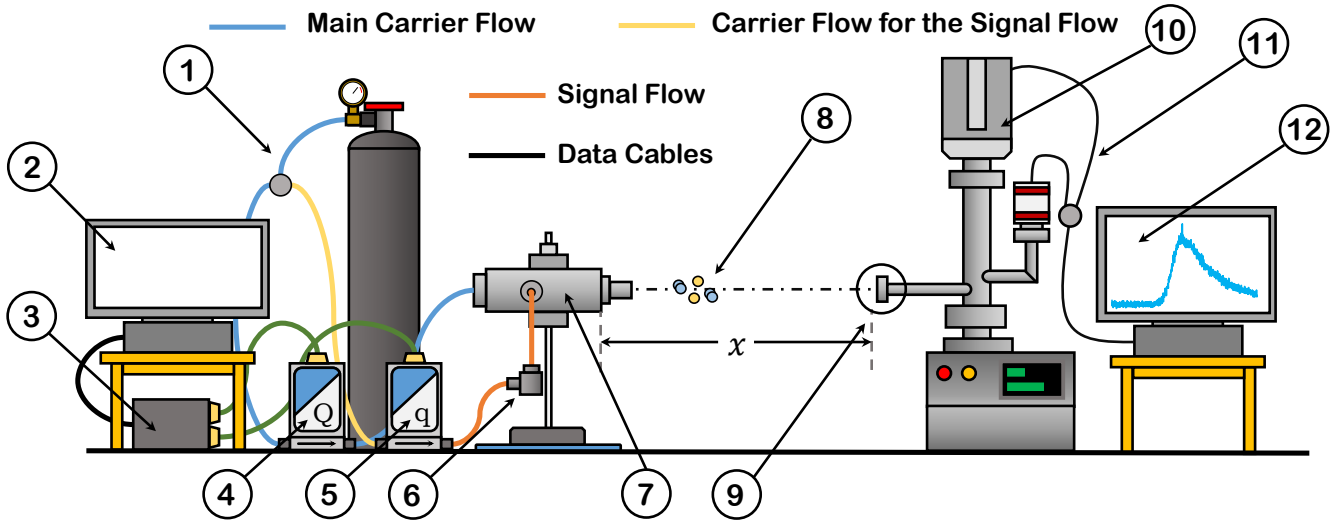

FIGURE 1: The diagram of the experimental setup: **(1)** (N_2) gas is used as the carrier flow (Q) and is transferred into the MFC that controls both the carrier flow (blue line) (Q) and the signal flow (yellow line) (q) **(2)** Information to be transmitted is generated using a computer **(3)** This information is transmitted into a modulation platform where the modulation chemicals are sent **(4)** MFC for the carrier flow **(5)** MFC for the signal flow **(6)** Evaporation Chamber (EC) where the signal chemical is injected **(7)** Mixing chamber where the signal chemicals arrive and initiate the transmission from the transmitter to the detector **(8)** Transmission medium **(9)** the inlet of the mass spectrometer **(10)** mass analyzer where the received chemical data is monitored **(11)** Controller for the vacuum pump of the mass spectrometer **(12)** Controller and the regulator cables for the mass spectrometer where the transmitted chemical data is recovered and analyzed.

A. TRANSMITTER

The transmitter, which can be seen in Figure 2, consists of three major parts. The first part consists of the mass flow controllers (MFC) that, depending on the message to be transmitted, closes and releases the valves that control the flow of the N_2 gas. This controlled gas then travels to the evaporation chamber (EC) where the evaporated chemicals in the chamber are carried over to the mixing chamber [34], [60]. For the experiment, volatile organic compounds (VOCs) are used. These types of chemicals have a high vapor pressure at room temperature because of the low boiling point of the chemicals.

The second part is the evaporation chamber (EC) where the sample is introduced. The chemicals are evaporated in the chamber and by using the MFC, a flow is generated and carried over to the last part of the transmitter, the mixing chamber.

B. CHEMICALS

In these experiments three types of chemicals were employed. A Zero-grade N_2 (% 99.998 purity) was chosen for the carrier gas (Q) that carries the signal chemical from the evaporation chamber to the transmitter and from the transmitter to the detector. The signal gas (q) was chosen to be acetone (% 99.8 purity, CAS Number: 67-64-1), which was diluted in methanol (over % 99.9 purity). The dilution in methanol produced a $\approx$ % 9 solution of concentration of the sample (1-part acetone, 10-part methanol). Both the acetone and methanol were introduced to the evaporation chamber (EC) in the liquid phase and N_2 was stored in the gas phase.

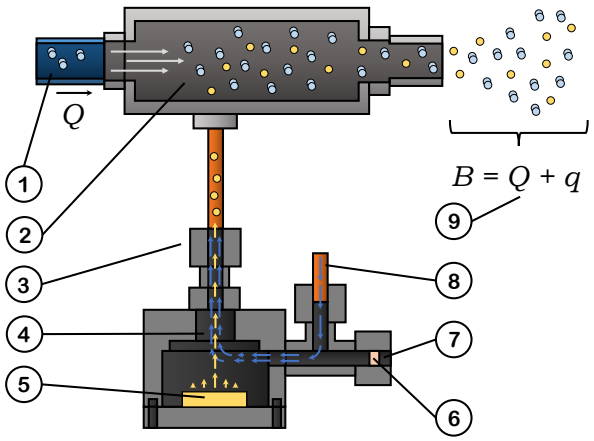

FIGURE 2: The working diagram of the odor generator along with the evaporation chamber (EC): **(1)** Introduction of the carrier gas (Q) into the mixing chamber **(2)** The evaporated chemicals from the chamber and the carrier gas are mixed in the chamber **(3)** The accumulated gas is transferred into the mixing chamber via a 0.25-inch Teflon tube **(4)** N_2 from the inlet carries the evaporated chemicals from the chamber **(5)** An absorptive material that holds the liquid sample analyte **(6)** thermo-resistant septum that allows the multiple introduction of a sample via a micro-syringe **(7)** Inlet where the sample is introduced **(8)** Inlet of the N_2 gas into the evaporation chamber **(9)** Transmitted chemicals that are released from the chamber.

C. DETECTOR

For the experiment, a portable membrane inlet mass spectrometer (MIMS), provided by Q Technologies Ltd., was used as the detector for the chemicals. The applications and the usage of the device are described in detail in the literature [61]–[65].

A MIMS is constructed from three primary components: a sampling probe, which allows the gas sample to penetrate the membrane to allow the MS to analyze; a triple filter quadrupole mass spectrometer (QMS), which is made from an electron ionization source (EI), a mass analyzer, a vacuum system and a detector. Finally, the inlet of the detector has a non-sterile flat polydimethylsiloxane (PDMS) membrane [34], [61].

The samples are introduced to the detector via a semi-permeable silicone membrane inlet sampling probe. The membrane is made from a non-sterile flat PDMS with a thickness of 0.12 mm and a sampling area of 33.2 mm^2.

III. MODELLING OF MACRO-SCALE MOLECULAR COMMUNICATIONS

A macro-scale molecular communication that utilizes particles as a means of conveying information can be modelled using the advection-diffusion equation [66], [67].

$$\frac{\partial C}{\partial t} = D\nabla^2 C - \nabla \cdot (\mathbf{u}C) + R \tag{1}$$

where C is the concentration of the transported mass in a given space and time (kg/m^3), D is the coefficient of diffusivity (cm^2/s), $\mathbf{u}$ is the velocity vector (cm/s) and R is the sink/source present in the environment. A simplified version of the equation can be derived by assuming that there are no sinks/sources ($R = 0$), constant diffusivity and the velocity having zero divergence ($\mathbf{u} \equiv 0$) . Since the area of the detector relative to the transmission distance is negligible, the main propagation element (advection) occurs in the x-direction and the diffusion in y and z axis (D_y, D_z) are assumed negligible based on the short distance of transmission ($x \ll 1\text{m}$), the equation given in Eq. (1) can be scaled back to 1D [38], [39].

$$\frac{\partial C}{\partial t} = D\frac{\partial^2 C}{\partial x^2} - u_x \frac{\partial C}{\partial x} \tag{2}$$

The solution, therefore, for the partial differential equation with an instantaneous (t = 0 s) and localized (x = 0 cm) for 1-D;

$$C(x,t) = \frac{M}{A_{yz}\sqrt{4\pi D_x t}} \exp\left(-\frac{\eta_x^2}{4Dt}\right) \tag{3}$$

where M is the mass introduced into the environment (g), D is the coefficient of diffusivity (cm^2/s), A_{yz} is the area-scale of the neglected dimensions. t is the duration of the experiment (s), C is the concentration of the chemical in 1-D (g/cm) and η_x is the moving reference frame in the x-direction with the following description.

$$\eta_x = x - (x_0 + u_x t) \tag{4}$$

where x_0 is the injection point of the chemicals into the environment and u_x is the advective flow in the x-direction. To model the molecular transmission, the detector is assumed to be ideal (zero detector delay and the chemicals introduced into the environment are absorbed into the detector given enough time) and the injection point of the chemical is defined as x_0 = 0. For a bit duration of T, the particle concentration of the bit value of '1' in 1-D can be expressed as;

$$C(x,t) = \frac{M}{\sqrt{4\pi Dt}} \exp\left(-\frac{\eta_x^2}{4Dt}\right) \tag{5}$$

Therefore, the particles that are absorbed by the detector $\theta_1(x,t)$ can be calculated by integrating the function with respect to the distance. This value is the particle quantity in

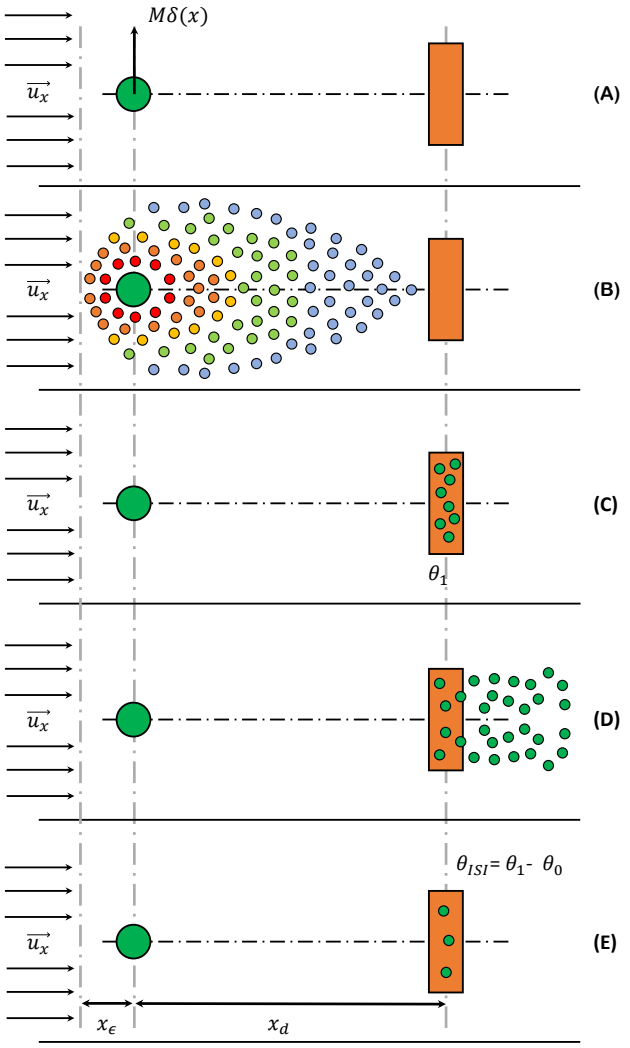

FIGURE 3: A diagram of the model used in the study **(A)** At t = 0 s mass is injected into the environment. This is defined by the initial boundary condition $C(x_0, t_0) = M\delta(x)$ **(B)** As the transmission evolves, the particles start propagating via advection and diffusion **(C)** When the specified period is passed the transmitter stops releasing particles and transmits only advective flow **(D)** The flow then forces the particles to be transferred from the detector to the outside environment **(E)** After a finite amount has passed the particles are removed from the detector and transferred to the outside environment. However, some particles are left in the detector, which can cause inter-symbol interference for future transmissions (θ_{ISI}).

a defined length $[x_\epsilon, x_d]$. By subtracting this value from the initial mass injected into the environment, particles that have been absorbed by the detector at position x_d can be calculated [38], [39], [59]. which is shown in Eq. (6) and (7).

$$\theta_1(x,t) = M - \int_{-x_\epsilon}^{x_d} C(x,t)\,dx \tag{6a}$$

$$\theta_1(x,t) = M - \int_{-x_\epsilon}^{x_d} \frac{M}{A_{yz}\sqrt{4\pi Dt}} \exp\left(-\frac{\eta_x^2}{4Dt}\right) dx \tag{6b}$$

$$\theta_1(x,t) = M - \frac{M}{2A_{yz}} \left[\text{erf}\left(\frac{x_d - u_x t}{2\sqrt{Dt}}\right) + \text{erf}\left(\frac{x_\epsilon + u_x t}{2\sqrt{Dt}}\right)\right] \tag{7}$$

where x_d is the distance from the injection point to the detector (cm) and the x_ϵ is the distance the chemicals travel that diffuse against the direction of the flow (cm). Because of the way diffusion occurs (i.e., Brownian process [68]) the possibility exists that the particles propagate in the opposite direction, against the advective flow. When the duration of the transmission is terminated for one bit symbol and 0 bit symbol transmission is initiated, the carrier flow (u_x) will start removing the chemicals present in the detector [38], [39]. The process of removal can be modelled by calculating the integration of the concentration function.

$$\theta_0(x,t) = \int_{-x_\epsilon}^{x_d} C(x,t)\,dx \tag{8a}$$

$$\theta_0(x,t) = \frac{M_R}{2A_{yz}} \left[\text{erf}\left(\frac{x_d - u_x t}{2\sqrt{D_x t}}\right) + \text{erf}\left(\frac{x_\epsilon + u_x t}{2\sqrt{D_x t}}\right)\right] \tag{8b}$$

However, since the time it takes for the detector to absorb all the chemicals in the environment (M_R) can take longer than the duration of the symbol bit, the particles that have been absorbed by the detector should be calculated. The remaining mass is calculated to be the difference between the introduction and the termination of the symbol.

$$M_R = \theta_1(x, nT) - \theta_1(x, T) \tag{9}$$

where n is the number of 1 bit symbol introduced into the system before the 0 bit transmission is initiated. It should be noted that the defining difference between the introduction (θ_1) and the removal (θ_0) of the chemicals in the detector is the mass value [39]. The derivation of the absobption/removal of the particles from the detector can be seen in more detail in [38] and the diagram of the model used in this study can be seen in Figure 3.

In this type of propagation, a measure of whether the transmission dominated by advection or diffusion can be characterised by the Peclet Number (dimensionless):

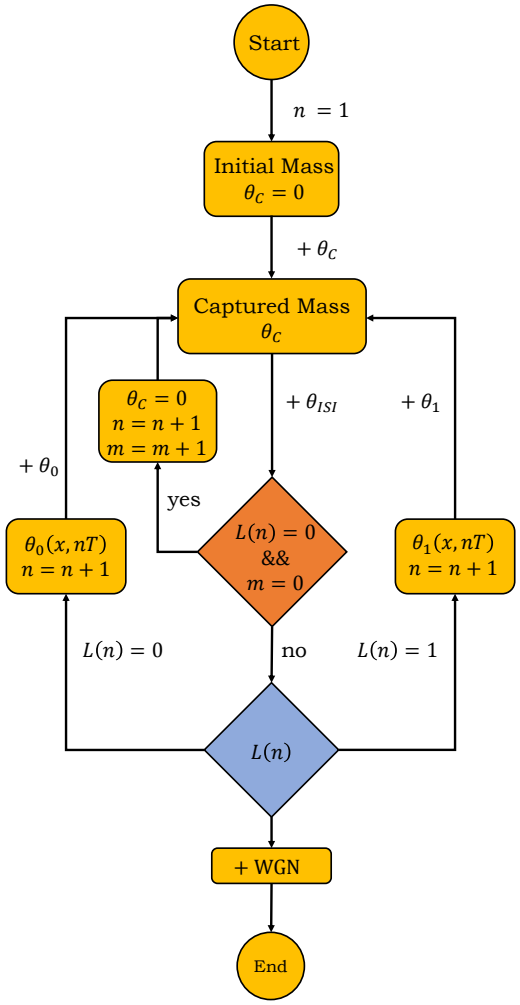

FIGURE 4: A diagram of the algorithm used in the simulation On-Off Keying (OOK) of macro-scale molecular communications

$$\text{Pe} = x_d \frac{u_x}{D} \tag{10}$$

For transmission with $\text{Pe} \ll 1$, the propagation is achieved mostly by diffusion. For $\text{Pe} \gg 1$, propagation is achieved by advective flow. Clearly as the transmission distance increases the propagation becomes advective dominant.

Based on the equation derived from Eq. (1), a simulation of the macro-scale molecular communications is developed. The flowchart for the simulation can be seen in Figure 4 and the description of the simulation is as follows;

1) A message array of $L(n)$ with a length of n is generated.
2) An initial definition of the captured mass (θ_C) is generated and given the value of $\theta_C = 0$ before any transmission commences.
3) The system checks the array to see if the first transmitted bit in the array is 0. This is done since the definition of the removal of particles (θ_0) relies on the mass that is absorbed by the detector (M_R), the removal of

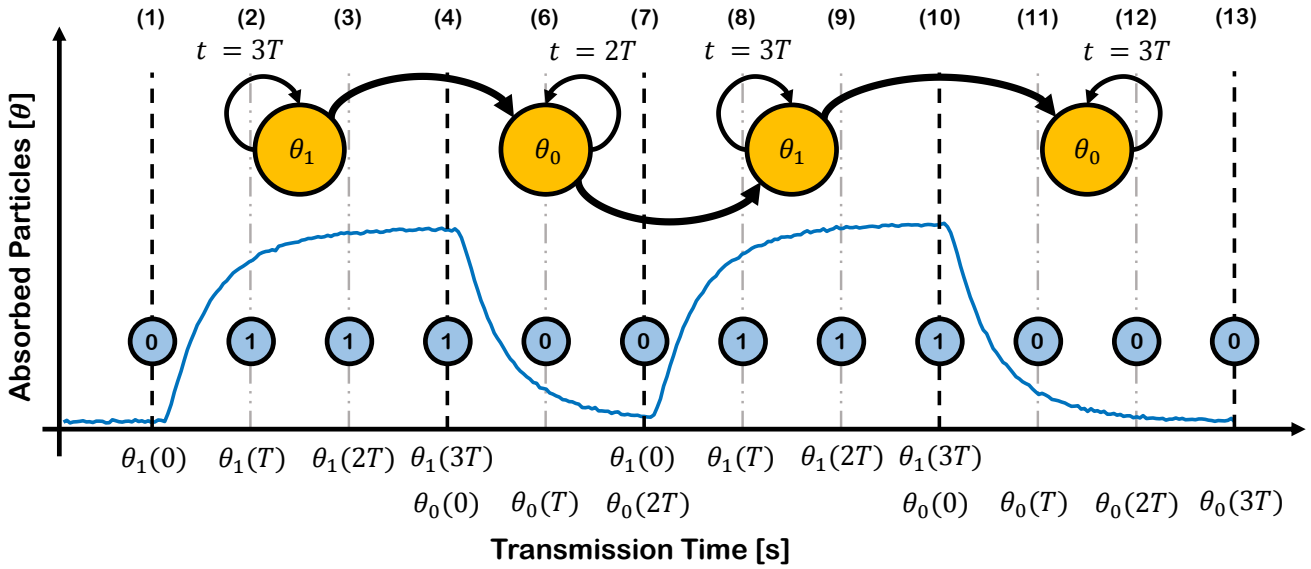

FIGURE 5: A representative diagram of how the transmission is simulated with an example transmission of a bit sequence of 011100111000 with states of the transmission shown above the transmission. The first part of the simulation is to analyze the sequence based on the states. In this context the states are defined as a bit value, which in this example are 0 and 1. In this example there are five states which are 0-1-0-1-0 with durations of $1T$-$3T$-$2T$-$3T$-$3T$. After this assessment the system carries out the following procedures to initiate the simulation. In this example at time-point **(1)**, the detector starts absorbing particles with the absorbing function θ_1 and this function continues until the time period of the state concludes at **(4)** in which the duration of the state is shown as the feedback loop to the state itself, with each bit-1 value having the absorbed mass value of $\theta_1(x, T)$, $\theta_1(x, 2T)$ and $\theta_1(x, 3T)$, respectively. When the time duration passes the time mark **(4)**, the removal function (θ_0) initiates and starts removing the particles from the detector based on how many particles it has absorbed in the previous state.

particles is not initiated and the captured mass value is stays $\theta_C = 0$ and the simulation continues to the next value in the array. This process continues until the system detects a 1 in the array ($L(n)$) and with each transmission of 0 bits in the array, moves the transmission window by the period of T. This check is carried out by the m parameter and once the simulation switches from 0 to 1 for the first time the m parameter is assigned the value of $m = 1$ and stops this loop until the termination of the simulation.

4) The system checks the bits in the array $L(n)$. If the bit value is 1, the system introduces the chemicals into the system. The duration of the bit-1 is dependent on how many bit-1s are present until a bit-0 is detected. For example, for a symbol duration of T with three bit-1s, the total mass accumulated by the system is $\theta_1(n, 3T)$ with each bit-1 value having $\theta_1(n, T)$, $\theta_1(n, 2T)$ and $\theta_3(n, 3T)$ respectively. This process can be seen in detail in Figure 5.
5) After the system has accumulated some particles from the bit-1 transmission, when the next bit is 0 the system flushes the chemicals relative to the particles already in the system and continues to remove the particles from the detector until a bit-1 is detected.($\theta_C = \theta_0$).
6) When the next bit-1 is to be transmitted, the leftover chemicals are added to the particle introduction $\theta_C = \theta_0 + \theta_1(x, nT)$.
7) The operation continues until the count operator (n) reaches the length of the message (L).
8) Before the simulation concludes, Additive White Gaussian Noise (AWGN) is added to the simulated signal [39].

In the following section the simulation will be compared to the experimental results gathered from the M-ary transmission study.

IV. M-ARY TRANSMISSION

M-ary transmission is a type of modulation in which multiple information bits are assigned to one transmission symbol. The experimental parameters of the M-ary transmission can be seen in Table 1. In the experiment 3 bit durations were tested: 30s, 60s and 90s. The message that was chosen for the transmission is 'MCX'. To quantify the signal correlation to the theoretical model, the Pearson correlation (ρ) is used with the following equation.

$$\rho_{E,T} = \frac{\text{cov}(E, T)}{\sigma_E \sigma_T} \tag{11}$$

where E is the experimental data and T is the theoretical data. The signal is sampled for all time samples.

A. 2-ARY TRANSMISSION

In 2-ary transmission, two levels of concentration are used in the transmission values and its corresponding bit values can be seen in Eq. (12).

$$\begin{aligned} \mathcal{X} &= \{0, 8\} \\ \mathcal{Y} &= \{0, 1\} \end{aligned} \tag{12}$$

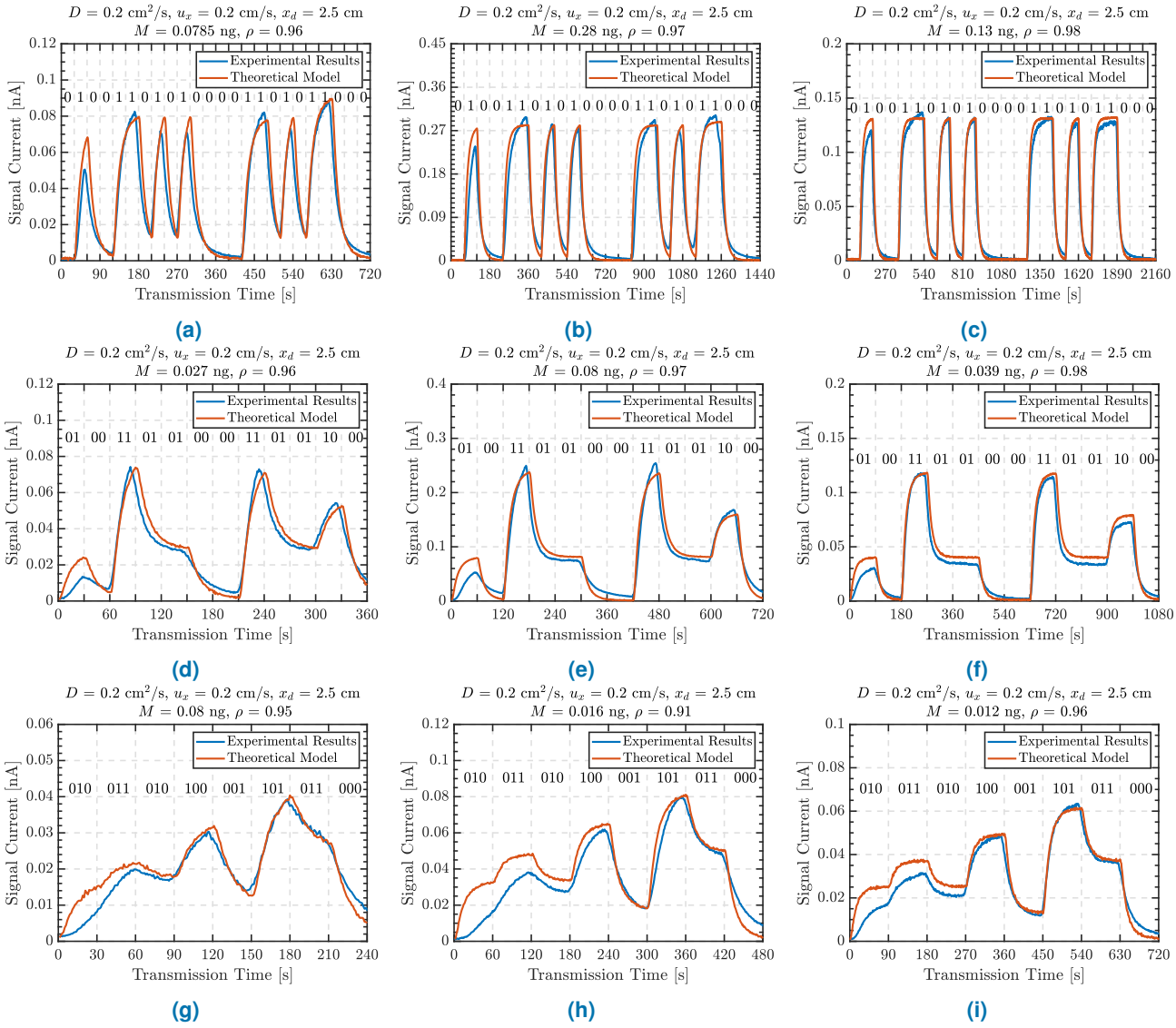

FIGURE 6: Experimental along with theoretical comparison of M-ary experiments (Noise Parameters: $\mu_N = 1.21 \times 10^{-3}$, $\sigma_N = 3.098 \times 10^{-4}$) **(a)** 2-ary transmission with bit duration of 30s **(b)** 2-ary transmission with bit duration of 60s **(c)** 2-ary transmission with bit duration of 90s **(d)** 4-ary transmission with bit duration of 30s **(e)** 4-ary transmission with bit duration of 60s **(f)** 4-ary transmission with bit duration of 90s **(g)** 8-ary transmission with bit duration of 30s **(h)** 8-ary transmission of with bit duration of 60s **(i)** 8-ary transmission with bit duration of 90s

TABLE 1: Experimental Parameters for the M-ary transmission

Parameter	Symbol	Value	Unit
Tracked signal flow ion	m/z	43	Da
Carrier flow	Q	750	ml/min
Carrier flow pressure	P_F	1	bar
Vacuum pump pressure	P_V	1.95×10^{-6}	torr
Environment temperature	T_E	297.35 ± 1.5	K
Environment pressure	P_E	1 ± 0.003	bar
Transmission distance	x	2.5 ± 0.1	cm
Diffusivity of acetone in air	D	0.124	cm^2/s
Acetone detection delay [34]	t_d	15	s

The experimental results along with the comparison with the the theoretical model can be seen in Figures 6a, 6b and 6c. As can be seen, the distinction between the two states is discernible, even on the shortest bit duration and the theoretical model shows strong agreement with the experimental results. Even though the clarity between the bits is high, the throughput of the communication is low since only 1 bit is transmitted for a given bit duration. As can be seen in Figures 6a, 6b and 6c the initial bit pulse has less correlation than the following pulses. This effect can be caused by the membrane present in the inlet of the detector where the initial interaction of the membrane and the transmitted chemicals can interfere with the absorbed mass by the detector. However as the transmission evolves the correlation of the theoretical model and the experimental results show high correlation.

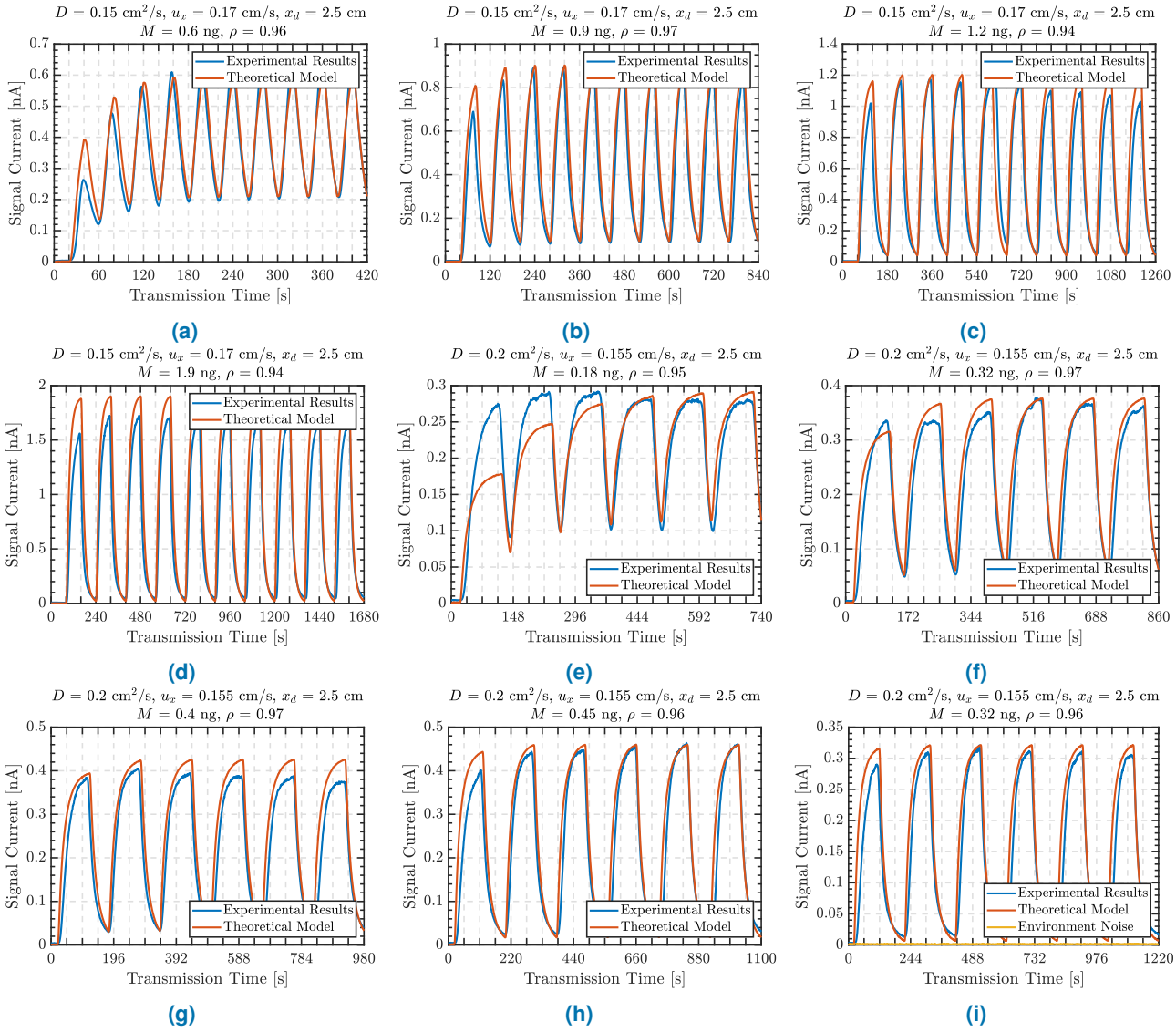

FIGURE 7: Results along with theoretical comparison of k **(a-d)** and one-to-zero **(e-i)** experiments (Noise Parameters: μ_N = 1.21 $\times 10^{-3}$, σ_N = 3.098$\times 10^{-4}$): **(a)** Bit transmission of 01 pairs **(b)** Bit transmission of 0011 pairs **(c)** Bit transmission of 000111 pairs **(d)** Bit transmission of 00001111 pairs **(e)** Bit transmission of 11111011111 pairs **(f)** Bit transmission of 111110011111 pairs **(g)** Bit transmission of 1111100011111 pairs **(h)** Bit transmission of 111110000111111 pairs **(i)** Bit transmission of 111110000011111 pairs

B. 4-ARY TRANSMISSION

In 4-ary transmission, four levels of concentration are used in the transmission of each symbol. The values and corresponding bit values can be seen in Eq. (13).

$$\begin{aligned} \mathcal{X} &= \{0, 3, 6, 9\} \\ \mathcal{Y} &= \{00, 01, 10, 11\} \end{aligned} \tag{13}$$

The experimental results along with the comparison to the theoretical model can be seen in Figures 6d, 6e and 6f. The M = 4 level modulation transmission shows some detrimental effect due to doubling the bits transmitted in a given second. The signals of 60s and 90s bit duration show a clear distinction between levels; however, the level differences are smaller in the 30s transmission.

C. 8-ARY TRANSMISSION

In 8-ary transmission, eight levels of concentration are used in the transmission of each symbol and its corresponding bit values can be seen in Eq. (14). The results are shows in Figures 6g, 6h and 6i. As can be seen, the effect of increasing the transmitted bits per second from 2 to 3 has increased the ISI of the communication.

$$\begin{aligned} \mathcal{X} &= \{0, 1, 2, 3, 4, 5, 6, 7\} \\ \mathcal{Y} &= \{000, 001, 010, 011, 100, 101, 110, 111\} \end{aligned} \tag{14}$$

V. MOLECULAR INTER-SYMBOL INTERFERENCE (MOISI)

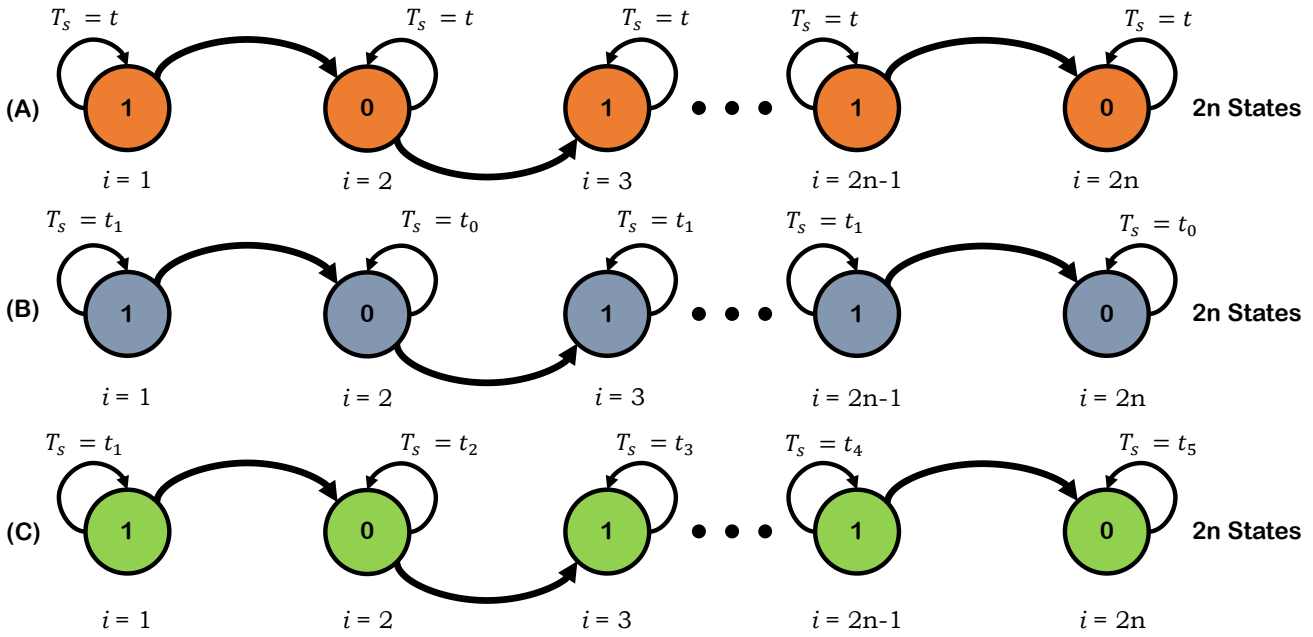

FIGURE 8: A diagram of possible transmissions that can create leftover chemicals (θ_{ISI}). In each sub-plot the bits are shown as circle diagrams and their duration is defined as T_S. In this model, shown in Section III, the bits are defined as the continuation of the θ function. For example, a transmission of 111 will have absorbed mass values of $\theta_1(x, T)$, $\theta_1(x, 2T)$ and $\theta_1(x, 3T)$, respectively. Based on this behaviour, each different bit is defined as a state (i) and can be seen in the sub-plots. **(A)** A sequential transmission of 1's and 0's continuously (i.e., 110011001100...) **(B)** A transmission of uneven amounts of 1's and 0's (i.e., 100010001001...) **(C)** A transmission where the transmission ends with chemical introduction into the environment (i.e., 101100011101111...)

TABLE 2: Experimental Parameters for Molecular (ISI) Study

Parameter	Symbol	Value	Unit
Tracked signal flow ion	m/z	43	Da
Signal flow	q	8	ml/min
Carrier flow	Q	750	ml/min
Carrier flow pressure	P_F	1	bar
Vacuum pump pressure	P_V	$2 \times 10^{-6} \pm 1 \times 10^{-6}$	torr
Environment temperature	T_E	299.35 ± 1.5	K
Environment pressure	P_E	1 ± 0.002	bar
Transmission distance	x	2.5 ± 0.1	cm
Diffusivity of acetone in air	D	0.124	cm^2/s

A. BIT-RATIO EXPERIMENTS

To understand the behaviour of the symbol transmission and the leftover chemical it leaves in the detector, a series of experiments were conducted. In these experiments a sequence of symbols were transmitted. The experimental parameters for the experiments can be seen in Table 2.

The first set of experiments was conducted by sending equal amounts of 1's and 0's (k = 1 is 101010..., k = 2 is 11001100..., k = 3 is 111000111... etc.).

The second set of experiments were conducted by sending a single 0 bit between an increasing amount of 1s (o/z = 1 is 10101..., o/z = 2 is 11011011... etc.).

1) k Experiments

The experimental results of sending equal amounts of 1s and 0s can be seen in Figures 7a, 7b, 7c and 7d. It is clear that when a bit sequence of 101010... is transmitted, the detector takes time to stabilize the background level. This is due to the way absorption and removal of particles inside the detector in which the behaviour is discussed in Section III.

When the transmitter introduces the particles into the detector, the absorption is based on the symbol duration in addition to the background noise, and when the advective flow clears out the particles from the detector, the flushing will be proportional to the particles already present in the detector. This flushing will increase when the detector has more particles, and this will continue until the amount of particles in the detector becomes high enough that the introduction (θ_1) and removal (θ_0) functions of the communication equalizes. However, when the transmitter introduces more particles before a flushing occurs, the detector needs fewer pairs to stabilize, which can be observed from Figures 7b to 7d.

2) One-to-Zero (o/z) Experiments

The results for the o/z can be seen from Figures 7e to 7i with an additional zero bit inserted between streams of 1-bits in each subsequent figure. It is clear that the more '0's are present in the transmission, the fewer particles are left in the detector, thereby decreasing the residual chemicals present and in o/z = 5 Figure 7i it is shown that the signal approaches the background noise level of the environment.

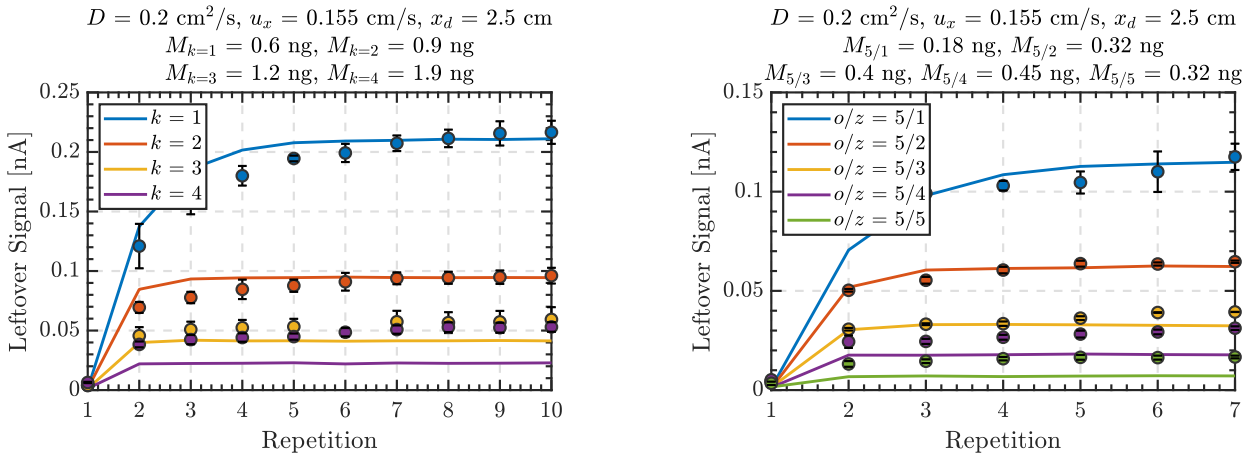

FIGURE 9: **(a)** Experimental results of the leftover chemicals from k experiment along with theoretical comparison **(b)** Experimental results of the o/z bit transmission with comparison to the theoretical model

B. RESIDUAL BACKGROUND SIGNAL

One of the important aspects of molecular communications is the leftover particles that decrease the amount of information that can be transmitted in a given symbol period. This property is unique to molecular communications. In electromagnetic (EM) communications, the interference is normally constant (i.e., N_0 stays stable). However, in this type of communication, the residual chemicals from 1-bit symbol can gradually increase the desired level and if the symbol duration is not kept at a reasonable duration, it will cause incorrect decoding. To model the ISI the equation derived in Eq. (7) is used. In this model the ISI can be modelled based on the interaction of the absorption (θ_1) and the removal (θ_0) of the particles. To simplify the equation, the part of the function where the absorption occurs is defined as;

$$U(x,t) = \left[\text{erf}\left(\frac{x_d - u_x t}{2\sqrt{D_x t}}\right) + \text{erf}\left(\frac{x_\epsilon + u_x t}{2\sqrt{D_x t}}\right)\right] \tag{15}$$

In the first part of the experiment (k study) equal numbers of bits ($U_1 = U_0$) were sent in sequence. A diagram of this kind of transmission can be seen in Figure 8 (A). Based on this bit transmission, the total ISI caused by the transmission can be expressed as;

$$\theta_{ISI} = M\sum_{i=1}^{i=n} U^i - \frac{M}{2}\sum_{i=1}^{i=n} U^{i+1} \tag{16}$$

In the second part of the experiment (o/z study) an uneven amount of 1's and 0's is sent in sequence ($U_1 \neq U_0$).The diagram for this transmission can be seen in Figure 8 (B). This change in transmission can be modelled as;

$$\theta_{ISI} = M\sum_{i=1}^{i=n} U_0^i - \frac{M}{2}U_1\sum_{i=1}^{i=n} U_0^i. \tag{17}$$

If the transmission has an even amount of state changes between bits 1 and 0, which can be seen in Figure 8 (C), the generalized equation that gives ISI is;

$$\theta_{ISI} = M\sum_{j=1}^{j=n}\prod_{i=j}^{i=n} U_{2i} - \frac{M}{2}\sum_{j=1}^{j=n} U_{2j-1}\prod_{i=j}^{i=n} U_{2i} \tag{18}$$

and if the transmission has an odd amount of state changes, the equation can be written by including an additional absorption (θ_1) value to Eq. (18).

$$\theta_{ISI} = M\sum_{j=1}^{j=n}\prod_{i=j}^{i=n} U_{2i} - \frac{M}{2}\sum_{j=1}^{j=n} U_{2j-1}\prod_{i=j}^{i=n} U_{2i} + M - \frac{M}{2}U_{2n+1} \tag{19}$$

The results of the leftover background-noise experiment compared to the theoretical model can be seen in Figures 9a and 9b for a k study and o/z study respectively. As can be seen, the model agrees well with the experimental data when the leftover particles from the transmission create a large amount of interference. However, as the chemicals create less and less interference, the model prediction becomes less accurate. This is due to the effect of the ambient noise playing a more important role. To mitigate the effect, an optimal time for the symbol period can be calculated based on the equations derived in Section III.

The optimal symbol period (OSP) can be calculated by maximizing the value in the error function erf(·). For the detector to retain no chemicals from transmission the error function must produce the value 1. However, due to the impracticality of this (erf(∞) = 1), a finite value must be chosen for the determination of the OSP. For a given value of n = 2 the error function produces the value of 0.995, which can be used for the practical cases of molecular communications.

By solving the error function present in the absorptions

equation given in Eq. (7) and Eq. (8b). As can be seen in both equations, there are two error functions main differences being the distance values; former being x_d and latter being x_ϵ. Since the distance that chemicals travel against the flow is negligible compared to the actual distance of the propagation ($x_d \gg x_\epsilon$) only the former part of the equation is used in calculation of the optimal sampling period. For a given n value the optimal symbol period (T_{OSP}) can be calculated as follows.

$$n = \left(\frac{x_d - u_x T_{\text{OSP}}}{2\sqrt{D T_{\text{OSP}}}} \right) \tag{20}$$

By solving the aforementioned equation with respect to T_{OSP} two solutions ($T_{\text{OSP}_1}, T_{\text{OSP}_2}$) can be derived which are presented below.

$$T_{\text{OSP}_1} = T_{\text{max}} = \frac{u_x x_d + 2Dn^2 + 2n\sqrt{D\left(Dn^2 + u_x x_d\right)}}{u_x^2} \tag{21a}$$

$$T_{\text{OSP}_2} = T_{\text{min}} = \frac{u_x x_d + 2Dn^2 - 2n\sqrt{D\left(Dn^2 + u_x x_d\right)}}{u_x^2} \tag{21b}$$

$$\theta_{ISI}(x,t) = \max\{\theta_c\} \quad \text{if} \quad T \leq T_{\text{min}} \tag{22a}$$

$$\theta_{ISI}(x,t) > 0 \quad \text{if} \quad T_{\text{min}} < T < T_{\text{max}} \tag{22b}$$

$$\theta_{ISI}(x,t) = \min\{\theta_c\} \quad \text{if} \quad T \geq T_{\text{max}} \tag{22c}$$

As long as the above criterion in Eq. (22) (c) not met, transmission will retain the ISI during the communication. The presence of the ISI will shift the distribution of 0 bits to a higher value as the transmission evolves, and if the receiver uses a static threshold detection (τ), it will increasingly decode 0 wrongly as the transmission continues and will create an uneven probability between $p(1|0)$ and $p(0|1)$, making the communication asymmetric.

VI. SYMBOL-ERROR RATE (SER)

To analyze the symbol-error rate (SER) properties of the macro-scale MC, an experiment was conducted, with the parameters of the experimental setup shown in Table 3. Bit durations of 5s, 10s, 15s and 20s are tested. Each experiment transmitted 100 bits, randomized with equal probabilities of 1s and 0s. In each experiment 300 μl of sample is introduced into the evaporation chamber (EC), then 5s, 10s, 15s and 20s experiments were made 3 times and the average error is taken. The experimental results along with the theoretical comparison of the SER can be seen in Figure 10.

It is clear that the experimental results show agreement with the numerical results obtained from the simulation with a correlation value of $\rho = 0.94$. A static threshold (τ) was used in the decoding of the received bits. The theoretical results of the SER graph of M-ary communication can be seen in Figure 12a. As can be seen with each additional information level in the symbol, the error rate increases for the same SNR value, and to compensate for the error, higher M-ary values needs higher SNR values.

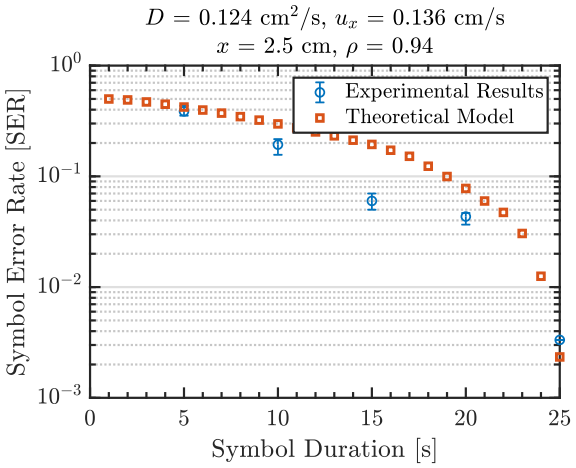

FIGURE 10: Experimental results of the symbol-error-rate (SER) and comparison to the theoretical model

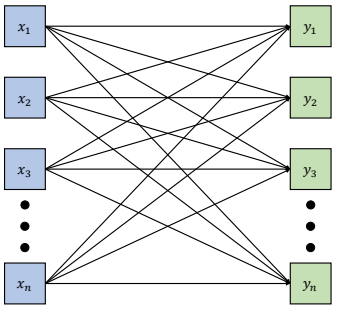

FIGURE 11: Representative diagram of a Binary Asymmetric Channel (BAC)

TABLE 3: Experimental Parameters for Bit Error Rate Experiment

Parameter	Symbol	Value	Unit
Tracked signal flow ion	m/z	43	Da
Signal flow	q	8	ml/min
Carrier flow	Q	750	ml/min
Carrier flow pressure	P_F	1	bar
Vacuum pump pressure	P_V	3.45×10^{-6}	torr
Environment temperature	T_E	299.35 ± 1.5	K
Environment pressure	P_E	1 ± 0.002	bar
Transmission distance	x	2.5 ± 0.1	cm
Diffusivity of acetone in air	D	0.124	cm^2/s

VII. CHANNEL CAPACITY

A. CHANNEL DEFINITION

When a 1-bit symbol is introduced to the detector, unless the symbol duration is shorter than the optimal given in Eq. (22)

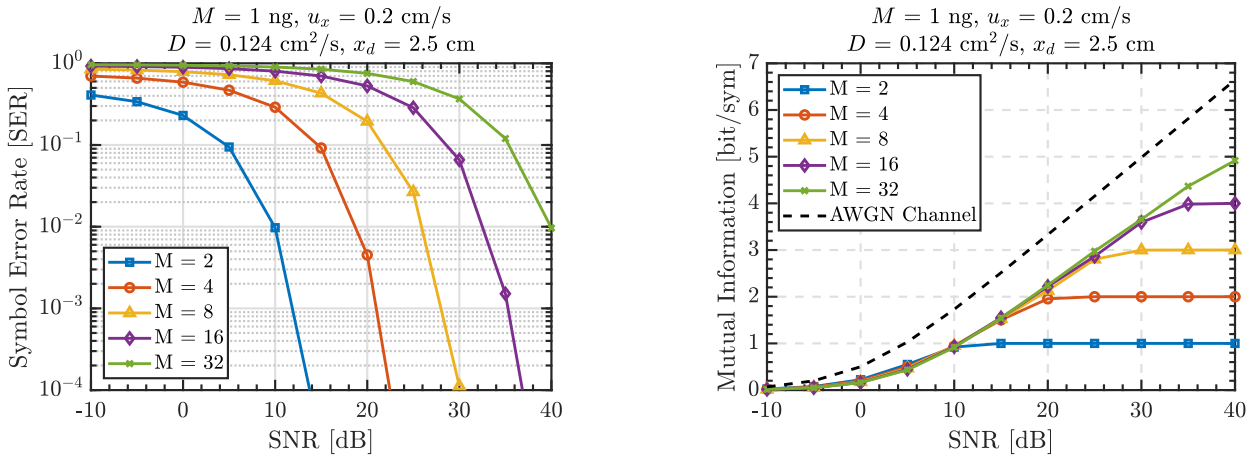

FIGURE 12: **(a)** Theoretical results of the Symbol-error rate of M-ary transmission **(b)** Theoretical results of the achievable information rate of M-ary transmission

(c), detector will absorb less mass than it was introduced into the environment. Moreover, since the flush mechanics relies on the particles that are already in the detector, the bit 0 cannot remove all the particles in the detector in the given time. Based on the ISI properties of the communication mentioned in the previous section, the communication channel can be expressed as asymmetric. The diagram of the channel can be seen in Figure 11.

To define the channel capacity, the mutual information ($I(\cdot;\cdot)$) must be measured. The channel capacity with a block length of n that possesses memory effects can be generalized to have the following equation [69];

$$C = \lim_{n\to\infty} \sup_{X^n} \frac{1}{n} I(X^n; Y^n) \tag{23}$$

The mutual information is a measure of how much one random variable tells about another with the definition of it given below [70].

$$I(X^n; Y^n) = H(Y^n) - H(Y^n|X^n) \tag{24}$$

where $H(Y^n)$ is the Shannon entropy of the probability vector Y and $H(Y^n|X^n)$ is the conditional entropy of Y given X. Based on the equations given in Eq. (23) and (24), the achievable mutual information is calculated by simulating the probabilities based on the simulation framework given in Section III.

VIII. THEORETICAL RESULTS

In this section of the study, three parameters of the transmission are studied for the symbol error rate (SER) analysis and the channel capacity. These parameters are: the transmission distance (x), the diffusivity (D) and the advective flow (u_x). Two types of comparisons were made. Firstly, a comparison was made by varying the signal-to-noise ratio (SNR) for both the SER and the channel capacity, and secondly the parameter (distance (x), advective flow (u_x) and diffusivity (D)) becomes the variable for the SER and the channel capacity to better observe the parameter effect on these communication properties. Finally, the AWGN channel capacity is plotted in conjunction with each parameter's mutual information plots in Figures 13a, 13b and 13c for the transmission distance, the coefficient of diffusivity and the advective flow, respectively. The achievable mutual information rate of the M-ary communication in a macro-scale molecular communication can be seen in Figure 12b.

A. TRANSMISSION DISTANCE

As can be seen in Figures 13d and 13a, as the transmission distance is increased, the attainable mutual information experiences a decrease and the number of errors in the communication sees an increase. This is caused by the insufficient time given for the detector to detect the particles. As distance increases, the duration of the propagation requires more time to travel and additionally the diffusive properties dilute the transmission, where the chemicals start propagating in directions other than the path of the advective flow, which increases the time needed to absorb all the chemicals in the medium. The effect of an increased transmission distance can be seen in Figures 13j and 13g.

B. COEFFICIENT OF DIFFUSIVITY

In Figures 13e and 13b, it can be seen that the increase in the diffusivity has a negligible effect on the SER and the MI. This could be due to the fact that with the presence of an advective flow, the effect of diffusion is suppressed, where the increase of the parameter plays a minor role. However, in Figures 13k and 13h, it can be seen that with an increase of the SNR the effects of diffusion becomes more noticeable and based on the simulation results, the effect seems to increase the mutual information. However, as stated, the effect is negligible.

C. ADVECTIVE FLOW

The effect of advective flow on the channel capacity can be seen in Figures 13f and 13c. As the velocity of the transmis-

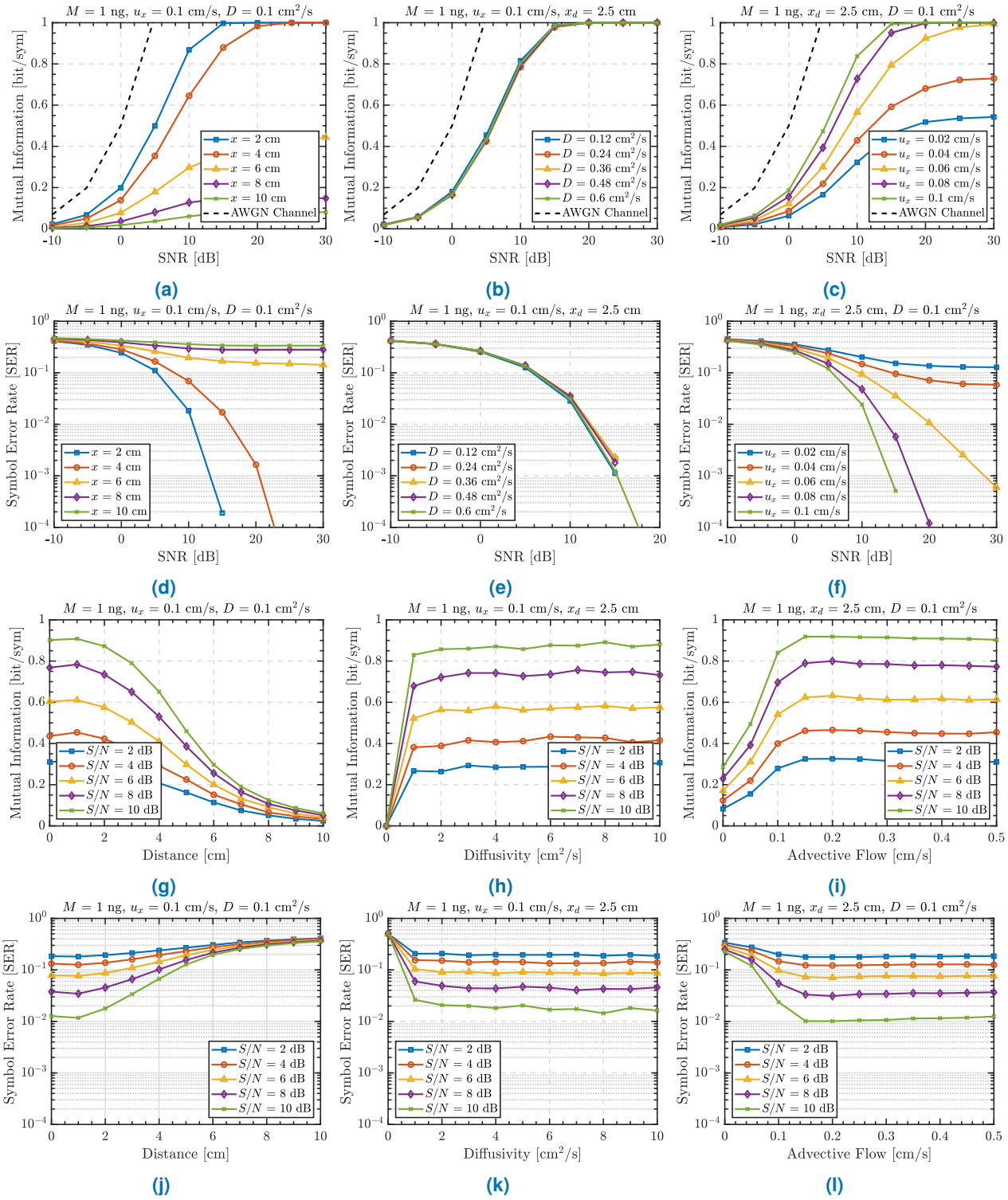

FIGURE 13: Theoretical analysis of achievable mutual information and SER of molecular communication **(a)** Achievable mutual information of different transmission distance (x) values with respect to Signal-to-Noise ratio (SNR) **(b)** Achievable mutual information of different coefficients of diffusivity (D) values with respect to Signal-to-Noise ratio (SNR) **(c)** Achievable mutual information of different advective flow (u_x) values with respect to Signal-to-Noise ratio (SNR) **(d)** SER of different transmission distance (x) values with respect to Signal-to-Noise ratio (SNR) **(e)** SER of different coefficients of diffusivity (D) values with respect to Signal-to-Noise ratio (SNR) **(f)** SER of different advective flow (u_x) values with respect to Signal-to-Noise ratio (SNR) **(g)** Achievable mutual information with increasing transmission distance **(h)** Achievable mutual information with increasing coefficients of diffusivity **(i)** Achievable mutual information with increasing advective flow **(j)** SER of different transmission distance (x) values **(k)** SER of different coefficients of diffusivity (D) values **(l)** SER of different advective flow (u_x) values

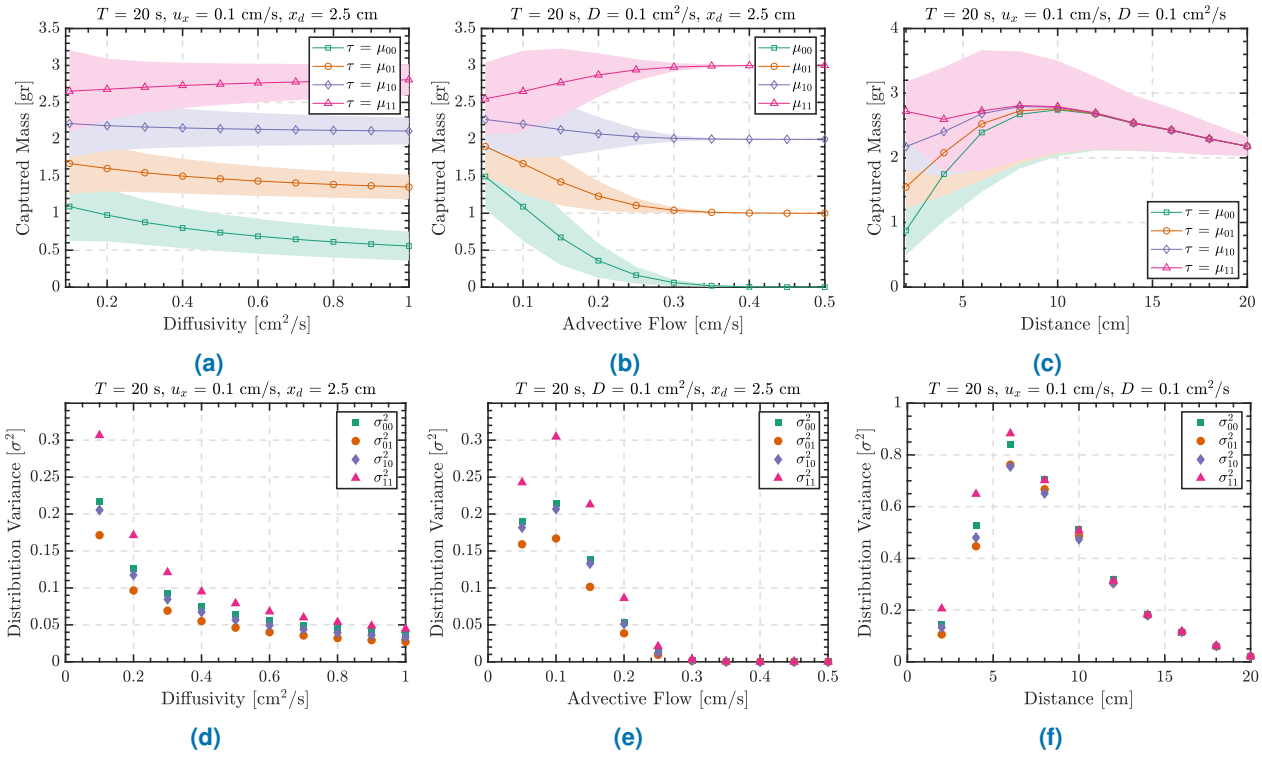

FIGURE 14: Simulation results of the symbol distribution of the transmitted symbol. In the plot μ are the mean value of the received mass of their respective symbol (00, 01, 10, 11) **(a), (b), (c)** and the symbol variance **(d), (e), (f)** of the following parameters: Diffusivity **(a), (d)**; Advective flow **(b), (e)**; Transmission distance **(c), (f)**

sion is increased, the channel capacity sees an increase with a corresponding decrease in errors. This is caused by the effect of advection rather than the effect of diffusion. The effect of advection has a greater increase on the channel capacity than the diffusion. The effect of increasing the advective flow on the increase of the mutual information and the reduction of the symbol errors can be seen in Figures 13i and 13l.

IX. DISTRIBUTION OF RECEIVED SYMBOL VALUES

To analyze the symbol distribution of molecular communications, simulations were made by changing the properties of the propagation. These are the diffusivity, the advective flow and the transmission distance. The effect of these parameters will be analyzed by a 4-level transmission.

A. TRANSMISSION DISTANCE

One of the detrimental effects of molecular communication is the achievable distance of transmission (x). The advective flow (u_x) alone cannot compensate for an increase in distance, the detection of the chemicals is delayed or particles that are sent get misdirected from the transmission path and fewer particles arrive at the detector. Particles not arriving at the detector can be caused by numerous parameters, such as diffusivity of the transmitted particles, flow or particles present in the environment. The distribution of chemicals with the transmission distance can be seen in Figure 14c and the variance can be seen in Figure 14f. As can be seen, the increase in distance causes the received mass value corresponding to symbol values to merge. This in turn causes a decrease in the correct decoding of the message and given enough distance eventually makes communication impossible.

B. ADVECTIVE FLOW

The effect of the flow on the symbol distribution can be seen in Figure 14b and the variance can be seen in Figure 14e. It is clear that the increase in flow plays a major role in the decrease in the variance (σ^2) of the distribution and the stability of the mean (μ) of the distribution. The results show that a small increase in the flow plays a substantial role in the separation of the symbols.

C. COEFFICIENT OF DIFFUSIVITY

Diffusivity is the action a particle takes by utilizing internal energy to propagate in a random fashion. Some particles will move against the direction of the flow, which causes a delay in the saturation and the flush of the signal, i.e., when a 1-bit symbol is introduced, the action of absorption takes longer as the diffusivity is increased. Because of this, the effect of increased diffusivity does not have such a profound effect on the decrease of the symbol distribution variance, as does the advective flow. The effect of diffusivity on the symbol distribution can be seen in Figure 14a and the variance can be seen in Figure 14d The results also show that increase advection is a much better choice for improving the detection of symbols than increasing the diffusivity.

X. CONCLUSION

This paper presents an experimental and analytical study on the M-ary transmission properties of macro-scale molecular communications. As a transmitter, an in-house-built odor generator was used and as a detector a mass spectrometer with a quadrupole mass analyzer (QMA) was utilized. M = 2, M = 4 and M = 8 level transmissions were made experimentally using a solution of acetone and methanol as the signal chemical. A simulation model was developed based on the advection-diffusion equation and was compared to experimentally detected signals. It was shown that the simulation agrees with the experimental results and that macro-scale molecular communication can be approximated by a simplified version of the 1D Advection-Diffusion Equation described in Section III. In addition, experimental results of the symbol error rate (SER) analysis of acetone on M = 2 level modulation, a theoretical analysis was made on the M = 4 and M = 8 level modulation along with a theoretical comparison of M = 2, which produced similar results to the experiment. A Binary Asymmetric Channel (BAC) was used to model the channel capacity and determine the optimum symbol rate for this particular macro molecular communications system. It was shown that the macro-scale molecular communication can be modelled and simulated using a variation of the advection-diffusion equation. In addition, parameters such as advective flow aids in terms of reducing the SER more than increasing the diffusivity coefficient and the distance at which transmission takes place has a detrimental effect on the channel capacity of the system. An in-depth analysis into Mo-ISI was carried and by using the model developed in Section III it was shown that the model is able to replicate the experimental results. From the model equations were derived that allow calculations of the ISI in a given transmission. Based on the model discussed in Section III, the bit distribution of the transmission is studied for three parameters and their effects were discussed. Future-work will focus on multi-molecular communication at the macro-scale.

ACKNOWLEDGMENT

The research was funded from the Engineering and Physical Sciences Research Council (EPSRC) under the grant agreement: EP/M029425/1 'Creating a Stink - Investigating Olfactory Transport Streams'.

REFERENCES

[1] W. C. Agosta, Chemical communication: the language of pheromones. Henry Holt and Company, 1992.
[2] J. Billen and E. D. Morgan, "Pheromone communication in social insects: sources and secretions," 1998.
[3] K. N. Slessor, M. L. Winston, and Y. Le Conte, "Pheromone communication in the honeybee (apis mellifera l.)," Journal of chemical ecology, vol. 31, no. 11, pp. 2731–2745, 2005.
[4] W. R. Loewenstein and B. Rose, "Calcium in (junctional) intercellular communication and a thought on its behavior in intracellular communication," Annals of the New York Academy of Sciences, vol. 307, no. 1, pp. 285–307, 1978.
[5] D. Bray, "Signaling complexes: biophysical constraints on intracellular communication," Annual review of biophysics and biomolecular structure, vol. 27, no. 1, pp. 59–75, 1998.
[6] M. J. Sanderson, A. Charles, and E. R. Dirksen, "Mechanical stimulation and intercellular communication increases intracellular ca2+ in epithelial cells." Cell regulation, vol. 1, no. 8, pp. 585–596, 1990.
[7] T. Nakano, A. W. Eckford, and T. Haraguchi, Molecular communication. Cambridge University Press, 2013.
[8] A. O. Bicen and I. F. Akyildiz, "System-theoretic analysis and least-squares design of microfluidic channels for flow-induced molecular communication," IEEE Transactions on Signal Processing, vol. 61, no. 20, pp. 5000–5013, 2013.
[9] T. Nakano, Y. Okaie, and J.-Q. Liu, "Channel model and capacity analysis of molecular communication with brownian motion," IEEE communications letters, vol. 16, no. 6, pp. 797–800, 2012.
[10] M. Ş. Kuran, H. B. Yilmaz, T. Tugcu, and B. Özerman, "Energy model for communication via diffusion in nanonetworks," Nano Communication Networks, vol. 1, no. 2, pp. 86–95, 2010.
[11] M. S. Leeson and M. D. Higgins, "Forward error correction for molecular communications," Nano Communication Networks, vol. 3, no. 3, pp. 161–167, 2012.
[12] C. Bai, M. S. Leeson, and M. D. Higgins, "Minimum energy channel codes for molecular communications," Electronics Letters, vol. 50, no. 23, pp. 1669–1671, 2014.
[13] M. U. Mahfuz, D. Makrakis, and H. T. Mouftah, "Performance analysis of convolutional coding techniques in diffusion-based concentration-encoded pam molecular communication systems," BioNanoScience, vol. 3, no. 3, pp. 270–284, 2013.
[14] ——, "On the characterization of binary concentration-encoded molecular communication in nanonetworks," Nano Communication Networks, vol. 1, no. 4, pp. 289–300, 2010.
[15] M. S. Kuran, H. B. Yilmaz, T. Tugcu, and I. F. Akyildiz, "Modulation techniques for communication via diffusion in nanonetworks," in Communications (ICC), 2011 IEEE International Conference on. IEEE, 2011, pp. 1–5.
[16] M. Ş. Kuran, H. B. Yilmaz, T. Tugcu, and I. F. Akyildiz, "Interference effects on modulation techniques in diffusion based nanonetworks," Nano Communication Networks, vol. 3, no. 1, pp. 65–73, 2012.
[17] B. Tepekule, A. E. Pusane, H. B. Yilmaz, and T. Tugcu, "Energy efficient isi mitigation for communication via diffusion," in Communications and Networking (BlackSeaCom), 2014 IEEE International Black Sea Conference on. IEEE, 2014, pp. 33–37.
[18] H. Arjmandi, A. Gohari, M. N. Kenari, and F. Bateni, "Diffusion-based nanonetworking: A new modulation technique and performance analysis," IEEE Communications Letters, vol. 17, no. 4, pp. 645–648, 2013.
[19] Y. Chahibi, M. Pierobon, S. O. Song, and I. F. Akyildiz, "A molecular communication system model for particulate drug delivery systems," IEEE Transactions on Biomedical Engineering, vol. 60, no. 12, pp. 3468–3483, 2013.
[20] Y. Chahibi and I. F. Akyildiz, "Molecular communication noise and capacity analysis for particulate drug delivery systems," IEEE Transactions on Communications, vol. 62, no. 11, pp. 3891–3903, 2014.
[21] U. Okonkwo, R. Malekian, B. Maharaj, and A. Vasilakos, "Molecular communication and nanonetwork for targeted drug delivery: A survey," IEEE Commun. Surveys & Tutorials, pp. 1–1, 2017.
[22] Y. Moritani, S. Hiyama, and T. Suda, "Molecular communication for health care applications," in Pervasive Computing and Communications Workshops, 2006. PerCom Workshops 2006. Fourth Annual IEEE International Conference on. IEEE, 2006, pp. 5–pp.
[23] L. Felicetti, M. Femminella, G. Reali, and P. Liò, "Applications of molecular communications to medicine: A survey," Nano Communication Networks, vol. 7, pp. 27–45, 2016.
[24] U. A. Chude-Okonkwo, "Diffusion-controlled enzyme-catalyzed molecular communication system for targeted drug delivery," in Global Communications Conference (GLOBECOM), 2014 IEEE. IEEE, 2014, pp. 2826–2831.
[25] B. Atakan, "Molecular communication among nanomachines," in Molecular Communications and Nanonetworks. Springer, 2014, pp. 1–24.
[26] S. F. Bush, Nanoscale communication networks. Artech House, 2010.
[27] R. A. Freitas, Nanomedicine, volume I: basic capabilities. Landes Bioscience Georgetown, TX, 1999, vol. 1.

[28] M. Cole, J. Gardner, S. Pathak, T. Pearce, and Z. Rácz, "Towards a biosynthetic infochemical communication system," Procedia Chemistry, vol. 1, no. 1, pp. 305–308, 2009.
[29] S. B. Olsson, L. S. Kuebler, D. Veit, K. Steck, A. Schmidt, M. Knaden, and B. S. Hansson, "A novel multicomponent stimulus device for use in olfactory experiments," Journal of neuroscience methods, vol. 195, no. 1, pp. 1–9, 2011.
[30] M. Cole, J. Gardner, Z. Ráczu, S. Pathak, T. Pearce, J. Challiss, D. Markovic, A. Guerrero, L. Muñoz, G. Carot et al., "Biomimetic insect infochemical communication system," in Sensors, 2009 IEEE. IEEE, 2009, pp. 1358–1361.
[31] L. Muñoz, N. Dimov, G. Carot-Sans, W. P. Bula, A. Guerrero, and H. J. Gardeniers, "Mimicking insect communication: Release and detection of pheromone, biosynthesized by an alcohol acetyl transferase immobilized in a microreactor," PloS one, vol. 7, no. 11, p. e47751, 2012.
[32] R. K. Vander Meer, M. D. Breed, K. E. Espelie, and M. L. Winston, "Pheromone communication in social insects," Ants, wasps, bees and termites. Westview, Boulder, CO, vol. 162, 1998.
[33] N. Farsad, W. Guo, and A. W. Eckford, "Tabletop molecular communication: Text messages through chemical signals," PloS one, vol. 8, no. 12, p. e82935, 2013.
[34] S. Giannoukos, A. Marshall, S. Taylor, and J. Smith, "Molecular communication over gas stream channels using portable mass spectrometry," Journal of The American Society for Mass Spectrometry, vol. 28, no. 11, pp. 2371–2383, 2017.
[35] S. Giannoukos, D. T. McGuiness, A. Marshall, J. Smith, and S. Taylor, "A chemical alphabet for macromolecular communications," Analytical Chemistry, vol. 90, no. 12, pp. 7739–7746, 2018, pMID: 29847932. [Online]. Available: https://doi.org/10.1021/acs.analchem.8b01716
[36] N. Farsad, D. Pan, and A. Goldsmith, "A novel experimental platform for in-vessel multi-chemical molecular communications," in GLOBECOM 2017-2017 IEEE Global Communications Conference. IEEE, 2017, pp. 1–6.
[37] H. Unterweger, J. Kirchner, W. Wicke, A. Ahmadzadeh, D. Ahmed, V. Jamali, C. Alexiou, G. Fischer, and R. Schober, "Experimental molecular communication testbed based on magnetic nanoparticles in duct flow," arXiv preprint arXiv:1803.06990, 2018.
[38] D. T. McGuiness, S. Giannoukos, A. Marshall, and S. Taylor, "Parameter analysis in macro-scale molecular communications using advection-diffusion," IEEE Access, 2018.
[39] ——, "Experimental results on the open-air transmission of macro-molecular communication using membrane inlet mass spectrometry," IEEE Communications Letters, vol. 22, no. 12, pp. 2567–2570, Dec 2018.
[40] J. Crank, The mathematics of diffusion. Oxford university press, 1979.
[41] B. Atakan and O. B. Akan, "An information theoretical approach for molecular communication," in Bio-Inspired Models of Network, Information and Computing Systems, 2007. Bionetics 2007. 2nd. IEEE, 2007, pp. 33–40.
[42] ——, "On channel capacity and error compensation in molecular communication," in Transactions on computational systems biology X. Springer, 2008, pp. 59–80.
[43] ——, "Deterministic capacity of information flow in molecular nanonetworks," Nano Communication Networks, vol. 1, no. 1, pp. 31–42, 2010.
[44] D. Arifler, "Capacity analysis of a diffusion-based short-range molecular nano-communication channel," Computer Networks, vol. 55, no. 6, pp. 1426–1434, 2011.
[45] B. Atakan, "Optimal transmission probability in binary molecular communication," IEEE Communications Letters, vol. 17, no. 6, pp. 1152–1155, 2013.
[46] M. Pierobon, I. F. Akyildiz et al., "Diffusion-based noise analysis for molecular communication in nanonetworks," IEEE Transactions on Signal Processing, vol. 59, no. 6, pp. 2532–2547, 2011.
[47] M. Pierobon and I. F. Akyildiz, "Capacity of a diffusion-based molecular communication system with channel memory and molecular noise," IEEE Transactions on Information Theory, vol. 59, no. 2, pp. 942–954, 2013.
[48] M. Turan, T. Tugcu, and H. B. Yilmaz, "Performance analysis of power adjustment methods in molecular communication via diffusion," in 2018 26th Signal Processing and Communications Applications Conference (SIU). IEEE, 2018.
[49] B. Yin and M. Peng, "Performance analysis of cooperative relaying in diffusion-based molecular communication," in 2018 International Conference on Computing, Networking and Communications (ICNC). IEEE, 2018, pp. 752–756.
[50] R. Mosayebi, H. Arjmandi, A. Gohari, M. Nasiri-Kenari, and U. Mitra, "Receivers for diffusion-based molecular communication: Exploiting memory and sampling rate," IEEE Journal on Selected Areas in Communications, vol. 32, no. 12, pp. 2368–2380, 2014.
[51] A. Einolghozati, M. Sardari, and F. Fekri, "Relaying in diffusion-based molecular communication," in Information Theory Proceedings (ISIT), 2013 IEEE International Symposium on. IEEE, 2013, pp. 1844–1848.
[52] H. B. Yilmaz and C.-B. Chae, "Arrival modelling for molecular communication via diffusion," Electronics Letters, vol. 50, no. 23, pp. 1667–1669, 2014.
[53] W.-A. Lin, Y.-C. Lee, P.-C. Yeh, and C.-h. Lee, "Signal detection and isi cancellation for quantity-based amplitude modulation in diffusion-based molecular communications," in Global Communications Conference (GLOBECOM), 2012 IEEE. IEEE, 2012, pp. 4362–4367.
[54] G. Chang, L. Lin, and H. Yan, "Adaptive detection and isi mitigation for mobile molecular communication," IEEE transactions on nanobioscience, vol. 17, no. 1, pp. 21–35, 2018.
[55] H. Zhai, Q. Liu, A. V. Vasilakos, and K. Yang, "Anti-isi demodulation scheme and its experiment-based evaluation for diffusion-based molecular communication," IEEE transactions on nanobioscience, vol. 17, no. 2, pp. 126–133, 2018.
[56] R. Mosayebi, A. Gohari, M. Mirmohseni, and M. Nasiri-Kenari, "Type-based sign modulation and its application for isi mitigation in molecular communication," IEEE Transactions on Communications, vol. 66, no. 1, pp. 180–193, 2018.
[57] P.-J. Shih, C.-h. Lee, and P.-C. Yeh, "Channel codes for mitigating intersymbol interference in diffusion-based molecular communications," in Global Communications Conference (GLOBECOM), 2012 IEEE. IEEE, 2012, pp. 4228–4232.
[58] D. T. McGuiness, A. Marshall, S. Taylor, and S. Giannoukos, "Asymmetrical Inter-Symbol interference in Macro-Scale molecular communications," in 5th ACM International Conference on Nanoscale Computing and Communication 2018 (ACM NanoCom'18), Reykjavik, Iceland, Sep. 2018.
[59] S. Wang, W. Guo, S. Qiu, and M. D. McDonnell, "Performance of macro-scale molecular communications with sensor cleanse time," in Telecommunications (ICT), 2014 21st International Conference on. IEEE, 2014, pp. 363–368.
[60] M. Statheropoulos, G. Pallis, K. Mikedi, S. Giannoukos, A. Agapiou, A. Pappa, A. Cole, W. Vautz, and C. P. Thomas, "Dynamic vapor generator that simulates transient odor emissions of victims entrapped in the voids of collapsed buildings," Analytical chemistry, vol. 86, no. 8, pp. 3887–3894, 2014.
[61] S. Giannoukos, B. Brkić, S. Taylor, and N. France, "Membrane inlet mass spectrometry for homeland security and forensic applications," Journal of the American Society for Mass Spectrometry, vol. 26, no. 2, pp. 231–239, 2015.
[62] S. Giannoukos, B. Brkić, and S. Taylor, "Analysis of chlorinated hydrocarbons in gas phase using a portable membrane inlet mass spectrometer," Analytical Methods, vol. 8, no. 36, pp. 6607–6615, 2016.
[63] S. Giannoukos, B. Brkić, S. Taylor, A. Marshall, and G. F. Verbeck, "Chemical sniffing instrumentation for security applications," Chemical reviews, vol. 116, no. 14, pp. 8146–8172, 2016.
[64] S. Giannoukos, B. Brkić, S. Taylor, and N. France, "Monitoring of human chemical signatures using membrane inlet mass spectrometry," Analytical chemistry, vol. 86, no. 2, pp. 1106–1114, 2013.
[65] S. Maher, F. Jjunju, I. Young, B. Brkic, and S. Taylor, "Membrane inlet mass spectrometry for in situ environmental monitoring," Spectrosc. Eur, vol. 26, pp. 6–8, 2014.
[66] C. E. Baukal Jr, V. Gershtein, and X. J. Li, Computational fluid dynamics in industrial combustion. CRC press, 2000.
[67] A. Bejan, Convection heat transfer. John wiley & sons, 2013.
[68] R. P. Feynman, R. B. Leighton, and M. Sands, The Feynman lectures on physics, Vol. I: The new millennium edition: mainly mechanics, radiation, and heat. Basic books, 2011, vol. 1.
[69] S. Verdú et al., "A general formula for channel capacity," IEEE Transactions on Information Theory, vol. 40, no. 4, pp. 1147–1157, 1994.
[70] T. M. Cover and J. A. Thomas, Elements of information theory. John Wiley & Sons, 2012.